

# PTCDA on Au(1 1 1), Ag(1 1 1) and Cu(1 1 1): Correlation of interface charge transfer to bonding distance

S. Duhm<sup>a</sup>, A. Gerlach<sup>b</sup>, I. Salzmann<sup>a</sup>, B. Bröker<sup>a</sup>,  
R.L. Johnson<sup>c</sup>, F. Schreiber<sup>b</sup>, N. Koch<sup>a,\*</sup>

<sup>a</sup> *Institut für Physik, Humboldt-Universität zu Berlin, Newtonstr. 15, D-12489 Berlin, Germany*

<sup>b</sup> *Institut für Angewandte Physik, Universität Tübingen, Auf der Morgenstelle 10, D-72076 Tübingen, Germany*

<sup>c</sup> *Institut für Experimentalphysik, Universität Hamburg, Luruper Chaussee 149, D-22761 Hamburg, Germany*

Received 29 June 2007; received in revised form 2 October 2007; accepted 10 October 2007

Available online 25 October 2007

## Abstract

The electronic structure at the interfaces of 3,4,9,10-perylene tetracarboxylic dianhydride (PTCDA) and the metal surfaces Au(1 1 1), Ag(1 1 1) and Cu(1 1 1) was investigated using ultraviolet photoelectron spectroscopy (UPS). By combining these results with recent X-ray standing wave data from PTCDA on the same substrates clear correlation between the electronic properties and the interface geometry is found. The charge transfer between the molecule and the metal increases with decreasing average bonding distance along the sequence Au–Ag–Cu. Clear signatures of charge-transfer-induced occupied molecular states were found for PTCDA on Ag(1 1 1) and Cu(1 1 1). As reported previously by Zou et al. [Y. Zou et al., *Surf. Sci.* 600 (2006) 1240] a new hybrid state was found at the Fermi-level ( $E_F$ ) for PTCDA/Ag(1 1 1), rendering the monolayer metallic. In contrast, the hybrid state for PTCDA/Cu(1 1 1) was observed well below  $E_F$ , indicating even stronger charge transfer and thus a semiconducting chemisorbed molecular monolayer. The hybridisation of molecular and Au electronic states could not be evidenced by UPS.

© 2007 Elsevier B.V. All rights reserved.

*PACS:* 73.61.Ph; 73.20.–r; 68.43.–h

*Keywords:* Organic/metal interface; Photoelectron spectroscopy; Energy level alignment; Charge transfer; Bonding distance; Electronic structure

## 1. Introduction

The energy level alignment at organic/metal interfaces is a key issue for the performance of

devices in the field of *organic electronics* [1,2]. Two rather simple models are often employed to describe limiting cases of the energy level alignment mechanism: (i) the Schottky–Mott limit, where the energies of the molecular orbitals (MOs) are strictly determined by the work function of the metal substrate involving vacuum level alignment, and (ii) Fermi-level pinning, where the energies of the

\* Corresponding author. Tel.: +49 30 2093 7819; fax: +49 30 2093 7632.

*E-mail address:* [norbert.koch@physik.hu-berlin.de](mailto:norbert.koch@physik.hu-berlin.de) (N. Koch).

MOs are pinned relative to the Fermi-level ( $E_F$ ) of the metal by charge transfer between the substrate and adsorbate [3,4]. However, these models do not incorporate the complex processes determining the energy level alignment at organic/metal interfaces, where other mechanisms like the chemical interaction between substrate and adsorbate [5,6], the electron push-back effect [1,7–9], interface dipoles [1,10,11], or the adsorption-induced geometry of the molecules [12–14] play important roles. Hence, in order to obtain a deeper understanding of energy level alignment mechanisms at organic/metal interfaces it is helpful to study the electronic interface properties of a structurally well characterized system.

An interesting model molecule in this context is 3,4,9,10-perylene tetracarboxylic dianhydride [PTCDA, Fig. 1]. The electronic as well as the geometric structure of PTCDA on different metal substrates has been studied in detail [15–28]. It is known that PTCDA can react strongly with metals *via* electron transfer [15–18], resulting in anionic molecular species. Despite the manifold possible interactions at the interface, PTCDA multilayers exhibit the same hole injection barrier (HIB) on a variety of polycrystalline metal substrates, covering a wide range of work functions (ca. 3.7–5.2 eV). For PTCDA on Mg, In, Sn and Au, [19] as well as for PTCDA on Au and Co, [20] the molecular levels have been investigated by ultraviolet photoelectron spectroscopy (UPS). For PTCDA on Au, Al and Sn the HIBs have been determined from current–voltage measurements in model devices [21]. Structural information for PTCDA adsorbed on single crystalline substrates Au(111), Ag(111) and Cu(111) has been obtained by means of low and high energy electron diffraction, scanning tunneling microscopy (STM) and X-ray diffraction [22,23,27,29]. Recent X-ray standing wave (XSW) studies have shown different adsorption geometries for PTCDA on Au(111) [12], Ag(111) [12–14] and

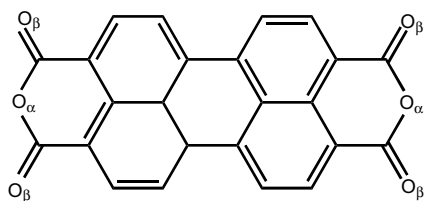


Fig. 1. Chemical structure of PTCDA, the indices mark the anhydride ( $O_\alpha$ ) and the carboxylic ( $O_\beta$ ) oxygen.

Cu(111) [14]. In addition to different average bonding distances of PTCDA on these metal surfaces, significant deviations from the planar bulk-conformation of the organic molecule were found. To obtain deeper insight in bonding mechanisms at organic/metal interfaces it is necessary to compare these data with the interfacial electronic structure of PTCDA on these three metal substrates. For PTCDA/Ag(111) it is already known that hybridisation of unoccupied and occupied molecular orbitals with Ag 4d-bands occurs in the monolayer [15,30], accompanied by electron transfer from the metal to the molecule. This well characterized system may act as a reference for PTCDA/Au(111), where the bonding is expected to be weaker than on Ag(111) [16,24,31] and for PTCDA/Cu(111) [27,28], where a stronger chemical interaction is expected [14,32]. We have performed UPS measurements on PTCDA/metal interfaces with Au(111), Ag(111), and Cu(111) substrates. These data reveal a correlation between the adsorption geometry and the interface electronic structure, leading to deeper insight into this interesting model system. In addition, the electronic structure of multilayer PTCDA has been measured on each substrate. Despite the remarkable differences in adsorption geometry and interfacial electronic structure for monolayers, the multilayer electronic structure and energy level alignment are virtually identical for all three cases.

## 2. Experimental details

Photoemission experiments were performed at the FLIPPER II end-station at HASYLAB (Hamburg, Germany) [33]. The interconnected sample preparation chambers (base pressure  $2 \times 10^{-9}$  mbar) and analysis chamber (base pressure  $2 \times 10^{-10}$  mbar) allowed sample transfer without breaking the ultrahigh vacuum. The Au(111), Ag(111) and Cu(111) single crystals were cleaned by repeated Ar-ion sputtering and annealing cycles (up to 550 °C). PTCDA was evaporated using resistively heated pinhole sources, at evaporation rates of about 1 Å/min. The film mass thickness was monitored with a quartz crystal microbalance. Hence, the values for PTCDA coverages corresponds to nominal film thicknesses. However, depending on the specific growth mode a nominal coverage of 2–3 Å corresponds to a monolayer on all three substrates. Spectra were recorded with a double-pass cylindrical mirror analyzer in off-normal

emission and an acceptance angle of  $24^\circ$  with an energy resolution of 200 meV and a photon energy of 22 eV. The secondary electron cut-offs (SECO) [for determination of the sample work function ( $\phi$ ) and the ionization energy] were measured with the sample biased at  $-3.00$  V. All preparation steps and measurements were performed at room temperature. The error of all given values of binding energies and SECO positions is estimated to  $\pm 0.05$  eV.

### 3. Results

The thickness dependent evolution of the photoemission spectra for PTCDA on the three different (111)-substrates is shown in Fig. 2.

The deposition of up to 2 Å PTCDA on Au(111) resulted in the attenuation of the Au derived photoemission features and the growth of a shoulder centered at 1.80 eV binding energy (BE) on the low

binding energy side of the Au 5d-bands. In analogy to earlier studies [31,34], we attribute this feature to the HOMO (highest occupied molecular orbital) of PTCDA. No indication for another molecular adsorption-induced photoemission feature close to  $E_F$  was found. Increasing the coverage up to 48 Å led to a continuous shift of this feature to 2.55 eV BE. At this multilayer coverage, the spectrum fully agrees with PTCDA spectra on polycrystalline Au reported previously [20,34]. For 1 Å PTCDA/Au(111) the sample work function decreased by 0.20 eV compared to pristine Au(111) ( $\phi_{\text{Au}} = 5.15$  eV), and by further 0.25 eV at a coverage of up to 48 Å (i.e.,  $-0.45$  eV total vacuum level shift).

For the Ag(111) substrate the deposition of 1 Å PTCDA resulted in several new photoemission features; a peak centered at 0.2 eV BE directly below the Fermi-edge of the metal ( $L'$ ) and another peak

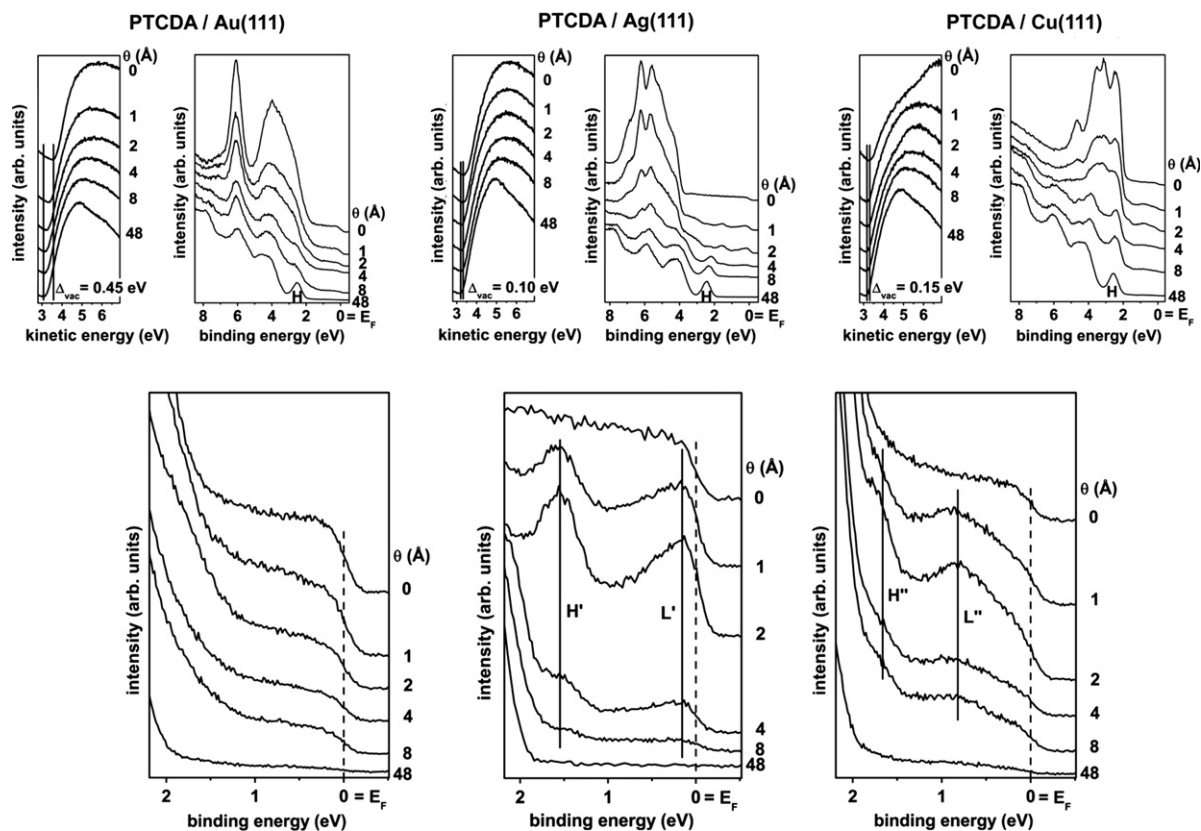


Fig. 2. Thickness dependent UPS spectra of PTCDA on Au(111), Ag(111) and Cu(111).  $\theta$  denotes the layer thickness. A coverage of about 3 Å corresponds to monolayer coverage. The first row displays in each case the secondary electron cut-off spectra and the survey spectra. H marks in each case the HOMO of multilayer PTCDA. The second row shows the corresponding spectrum in the region close to the Fermi-energy ( $E_F$ ) on an enlarged scale.  $H'$  marks the HOMO and  $L'$  the LUMO-derived interface states in the case of PTCDA/Ag(111),  $H''$  and  $L''$  the same for PTCDA/Cu(111).  $\Delta_{\text{vac}}$  denotes the decrease in the vacuum level between the pristine metal and multilayers of PTCDA.

centered at 1.55 eV BE ( $H'$ ). Increasing the coverage up to 2 Å led to enhanced intensity of both peaks. However, for 4 Å PTCDA coverage the intensity of the two peaks  $L'$  and  $H'$  decreased and a new peak centered at 2.20 eV BE emerged. Increasing the coverage up to the final value of 48 Å led to a shift of this peak to 2.45 eV BE, while the two low BE peaks vanished.  $\phi$  of pristine Ag(111) was 4.90 eV. For sub-monolayer coverage  $\phi$  decreased by only 0.10 eV and stayed constant for higher coverages.

The deposition of up to 2 Å PTCDA on Cu(111) also resulted in two new photoemission features in the region near to  $E_F$ , i.e., a broad peak centered at 0.80 eV BE ( $L''$ ) and another peak centered at 1.70 eV BE ( $H''$ ). At higher coverages the intensities of these peaks decreased and at 48 Å PTCDA coverage these peaks and the metal Fermi-edge were no longer visible. However, similar to the case of PTCDA/Ag(111) a new peak centered at 2.55 eV BE emerged at multilayer coverage.  $\phi$  of clean Cu(111) was 4.90 eV. The work function was decreased by 0.15 eV for a coverage of 1 Å PTCDA and stayed essentially constant for further PTCDA deposition.

The work function at monolayer coverage was 4.75 eV on all three substrates, regardless of the shape of the photoemission spectrum. The HOMO positions of all multilayer samples were virtually identical, with the peaks centered at 2.55 eV for PTCDA/Au(111) and PTCDA/Cu(111), and at 2.45 eV BE for PTCDA/Ag(111). Consequently, the PTCDA ionization energies (measured from the HOMO-onset to the vacuum-level) were identical on all three substrates within the error bar of  $\pm 0.05$  eV, namely 6.80 eV on Au(111), 6.85 eV on Ag(111) and 6.75 eV on Cu(111).

#### 4. Discussion

In the following we will discuss our photoemission results in the light of previous knowledge about the properties of PTCDA/metal interfaces. We will make particular relation to recently reported bonding distance values, which will finally allow to arrive at a comprehensive picture of PTCDA/metal interface energetics.

It has been suggested that the interaction between a conjugated organic molecule and a Au(111) surface should be rather weak [16,24]. Consequently, no clear signature of molecule-metal reaction-induced peaks within the energy gap region

of PTCDA was observed in the spectra of PTCDA/Au(111), even at sub-monolayer coverage (Fig. 2). The shift of the HOMO between monolayer and multilayer of 0.75 eV towards higher binding energies seems unusually large for weakly interacting conjugated organic molecules on metals. Usually, the screening of the photo-hole by the metal charge density results in shifts up to 0.40 eV between mono- and multilayer coverage of molecules on metals [35,36]. The position of the HOMO in the monolayer (1.80 eV BE) is in good agreement with scanning tunneling spectroscopy (STS) data, where a HOMO position of 1.90 eV BE was measured [24]. In contrast, another STS study found the HOMO centered at 2.18 eV BE for monolayer PTCDA/Au(111) and at 2.32 eV BE for 2–3 layers PTCDA/Au(111) [31]. As an explanation for this discrepancy, different tip–surface interactions and/or tunneling distances were suggested [24]. A monolayer of PTCDA on Au(111) forms well ordered domains with two distinct structures, but only modification is observed in the second and subsequent layers [37,38]. A recent STS study of the unoccupied states of PTCDA/Au(111) reported differences in the position of the lowest unoccupied molecular orbital (LUMO) of up to 0.35 eV depending on the adsorption domain of PTCDA [39]. The authors suggested hydrogen-bond-mediated intermolecular interaction to be responsible for the different peak positions. By analogy, differences of the same order of magnitude should be possible for occupied states. The area-averaged UPS spectra reveal both peaks, but the peak at higher BE may be masked by the dominant Au 5d emission. However, the differences in the electronic structure of the two monolayer adsorption domains, coupled with the polarization effect of the photo-hole can explain the 0.75 eV shift of the PTCDA HOMO between mono- and multilayer. UPS data of multilayer PTCDA on polycrystalline Au report the HOMO peak centered at 2.60 eV BE [34] or 2.35 eV BE [20], respectively. Considering the structural differences between Au(111) and polycrystalline Au, our value is in good agreement with the literature.

The absence of clear molecule-derived photoemission features in the energy gap region may thus be interpreted as indicative of physisorption of PTCDA on Au(111). However, the small decrease of  $\phi$  by only 0.45 eV induced by a monolayer of PTCDA on Au(111) compared to the pristine substrate may indicate a stronger interaction than only physisorption. The electron push-back effect fre-

quently leads to a larger decrease of  $\phi$  (in the range of 1 eV) for molecules physisorbed on Au surfaces [1,8]. Molecules chemisorbed on a metal via electron transfer (from the metal to the molecule) induce an additional contribution to the total interface dipole, which can partially or totally cancel the push back effect [6,40]. If the charge transfer for PTCDA/Au(111) were very small, the experimental observation would merely be limited by the fact that the newly induced density of states is simply too low to be detected [41]. Moreover, detailed theoretical work for PTCDA/Au(111) suggested significant molecular level broadening and interface electron density rearrangement induced by the metal proximity [42], which could be regarded as another way of describing a “soft” chemisorption process.

PTCDA on Ag(111) exhibits a strong chemical interaction, accompanied by electron transfer from Ag to PTCDA [15,16]. Following earlier reports, the (sub-)monolayer peaks in the energy gap of PTCDA are assigned to hybrid states of the Ag 4d-bands and the LUMO (now partially filled  $L'$ ), HOMO (now the  $H'$ ), and the HOMO-1 states of neutral PTCDA [15,30]. At elevated temperatures PTCDA/Ag(111) grows in the Stranski–Krastanov mode, but at room temperature the growth becomes more layer-by-layer like [43,44]. Consequently, these interface states are no longer visible in the UPS signal for higher PTCDA coverages. The LUMO-derived interface peak ( $L'$ ) is located directly at the Fermi-level, thus a monolayer PTCDA on Ag(111) is metallic [15]. The peak emerging at 2.20 eV BE at a coverage of 4 Å was assigned to the HOMO of neutral molecules [15]. The shift of the HOMO peak to 2.45 eV BE for 48 Å PTCDA coverage can be attributed to different polarization energies of PTCDA for the monolayer and multilayers [31]. The decrease in  $\phi$  between the pristine metal and monolayer PTCDA is much smaller than for PTCDA/Au(111), also indicative of a stronger chemical interaction between the substrate and the adsorbate.

The observation of interface states for a monolayer of PTCDA on Cu(111) shows that strong chemical interaction occurs at this interface. As the behavior of the SECO is similar to PTCDA/Ag(111), we conclude that significant electron transfer from the metal to the molecule takes place as well. Thus, peak  $L''$  is assigned to the (partially) filled LUMO and  $H''$  from the HOMO of the neutral PTCDA molecule. However, these interface states of PTCDA on Cu(111) are centered at signif-

icantly higher binding energies than for PTCDA/Ag(111). The energetic differences indicate that the hybridization of the molecular levels and the Cu 3d-bands is different from the case of PTCDA/Ag(111). Because the peaks are shifted to higher binding energies, stronger bonding of PTCDA to Cu(111) is likely. For monolayer PTCDA on Cu(111) the LUMO-derived interface state ( $L''$ ) is located clearly below the Fermi-level, i.e., a monolayer of PTCDA on Cu(111) is expected to be semiconducting, in contrast to the metallic molecular layer on Ag(111). Since PTCDA on Cu(111) grows in the Stranski–Krastanov mode [27], the interface state photoemission is not completely attenuated by overlayer material in the UPS spectra at multilayer coverages. The position of the HOMO of the multilayer is consistent with UPS data for PTCDA on polycrystalline Cu, where a HOMO position of 2.47 eV BE has been reported [20].

The electronic structure of PTCDA on the different substrates exhibits remarkable differences, ranging from “soft” chemisorption (on Au) to strong hybridization of metal bands and molecular orbitals, yielding metallic (on Ag) or semiconducting monolayers (on Cu). It is now interesting to see how these differences in the electronic structure are reflected in the adsorption geometry and bonding distance of PTCDA on the metal substrates (or, of course, *vice versa*). In Fig. 3 the binding models of PTCDA on Au(111), Ag(111) and Cu(111), are summarized schematically. The PTCDA energy levels in the interface region are compared to those in PTCDA multilayers (Fig. 3a) and the binding positions  $d_H$  of the carbon and oxygen atoms of PTCDA adsorbed on the three noble metals (Fig. 3b), using the results from X-ray standing wave studies [12–14].

The comparably weak PTCDA/Au(111) interaction is reflected in both the electronic structure and the adsorption geometry. In the UPS spectra no LUMO-derived features appeared at the PTCDA/Au(111) interface. The XSW results report an average carbon bonding distance of PTCDA on Au(111) ( $d_H = 3.27$  Å) [12] close to the molecular stacking distance measured in PTCDA single crystals ( $d_{(102)} = 3.22$  Å) [45], which also suggests a rather weak interaction. For PTCDA on Ag(111) a clear LUMO-derived peak ( $L'$ ) appeared in the interface region directly at the Fermi-edge, which leads to the metallic character of adsorbed PTCDA. The interface electronic structure of PTCDA on Ag(111) has already been discussed in detail

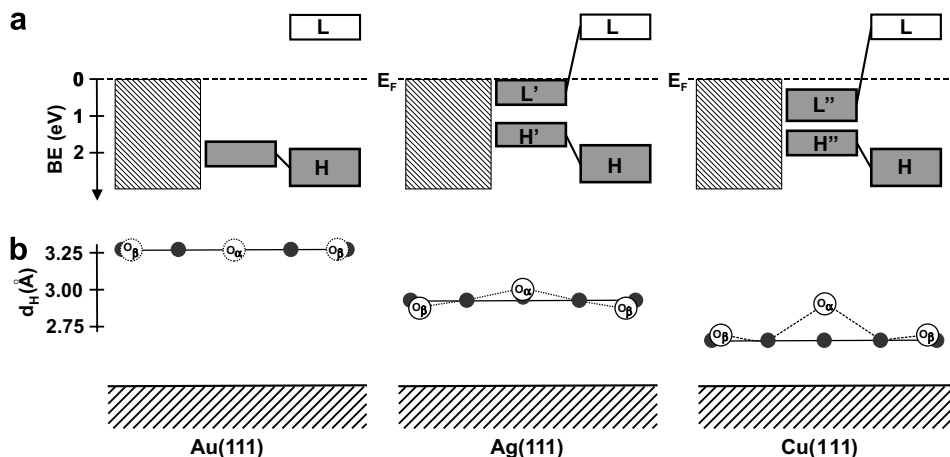


Fig. 3. (a) Schematic energy level diagram of PTCDA on Au(111), Ag(111) and Cu(111). The shaded area corresponds to the metal electron density, gray bars to occupied and open bars to unoccupied molecular orbitals. From left to right, the pristine metal, the interface region with the LUMO and HOMO derived interface states labeled L' and H' for the metallic case of PTCDA/Ag(111) and L'' and H'' for the semiconductive case of PTCDA/Cu(111) and multilayer PTCDA (H and L) are shown. The positions of the LUMOs are estimated from the transport gap, measured with (inverse) photoemission for PTCDA/Ag [31]. (b) Schematic binding positions of PTCDA on the three different substrates as measured in [12–14]. The position of the oxygen atoms in PTCDA/Au(111) was not measured with XSW, however a merely planar adsorption geometry of PTCDA on Au(111) might be assumed [22,23].

[15,30] and is presented here for completeness. The adsorption geometry with an average carbon bonding distance of  $d_H = 2.86 \text{ \AA}$  [13,14] directly supports the strong chemical interaction of PTCDA with Ag(111). In addition, PTCDA on Ag(111) shows a nonplanar adsorption geometry with the carboxylic oxygens ( $O_\beta$ ) bent towards and the anhydride oxygens ( $O_\alpha$ ) bent away from the metal surface with respect to the carbon plane. On the Cu(111) substrate the higher binding energy of the LUMO-derived peak (L'') compared to PTCDA/Ag(111) nicely correlates with the even smaller bonding distance of PTCDA carbons ( $d_H = 2.66 \text{ \AA}$ ) [14]. In addition, the PTCDA bending on Cu is also different than on Ag, as all of the oxygen atoms are bent away from the surface with respect to the PTCDA carbon plane.

Making an overall comparison of UPS and XSW results, a direct correlation between the adsorption geometry and strength of chemical bonding can be found. With increasing metal reactivity the chemical interaction, as revealed by the interfacial electronic structure, increases and the carbon bonding distance decreases accordingly. The distortion of the PTCDA molecules in the case of the strongly interacting systems PTCDA/Ag(111) and PTCDA/Cu(111) is not yet fully understood [14]. However, it can be speculated that the different molecular conformations (i.e., bending of the carboxylic oxygens) are directly related to the amount of charge trans-

ferred to the molecule, evidenced by the metallic-type monolayer PTCDA on Ag(111) and the semiconducting-type on Cu(111). This open question may be the topic of further ab initio calculations.

In the following, we consider the properties of the PTCDA multilayers on the three different substrates. The PTCDA ionization energies were found to be essentially the same on all three substrates. Despite the obvious differences in the (sub-)monolayer spectra, the hole injection barriers of multilayer PTCDA on all three substrates are virtually identical. Considering the work functions of PTCDA monolayers on the three substrates this finding is no longer surprising, since  $\phi$  for all three monolayer PTCDA/metal systems is the same. Particularly for PTCDA on Ag(111) and Cu(111) the chemisorbed monolayer must be regarded as a modified metal substrate for the multilayer growth. The molecular levels of PTCDA in the multilayer are thus aligned relative to the modified substrate  $\phi$  as in other organic heterostructures [6,46]. Therefore the observation of the nearly equal HIBs on all three substrates irrespective of the initial clean metal substrate work function cannot be interpreted in terms of “classical” Fermi-level pinning in the framework of organic/metal interfaces, where besides a small charge transfer between the metal and the adsorbate no chemical interaction occurs and a small density of interface states is able to pin the molecular orbitals [3,4]. Reactive PTCDA

is possibly a special case, which is not compatible with the existing energy level alignment models. The three-layer model (metal–chemisorbed monolayer–multilayer) can explain our findings, but the reason for the constant work functions of the PTCDA/metal systems remains open. An alternative approach may be provided by the calculations of charge neutrality levels (CNL) [42,47]. In the case of PTCDA on Au(111), a CNL level is found ( $2.45 \pm 0.10$ ) eV above the center of the PTCDA HOMO level, the CNL again is located 0.02 eV above  $E_F$  [42]. This result is in good agreement with our measured HOMO positions. Vázquez et al. [42,47] stated that changes in the bonding distance of PTCDA and distortions in the range of the experimentally measured values on the different substrates have no significant influence on the position of the CNL. Therefore, also for PTCDA/Ag(111) and PTCDA/Cu(111) the CNL theory should be applicable. It should be interesting to see in future work, whether this theory, which was designed for chemically weakly interacting systems, can successfully describe the physics at these interfaces.

## 5. Conclusion

We have demonstrated chemisorption with different interaction strength of PTCDA on the substrates Au(111), Ag(111) and Cu(111) using photoemission. Our results confirm the results from recent XSW studies and reveals the correlation between the strength of the chemical interaction and the average bonding distance. Taking PTCDA on Ag(111) as a reference we find that PTCDA binds more strongly to Cu(111) and less strongly to Au(111). For PTCDA on Au(111) no additional states are observed in the energy gap and the bonding distance is large. For PTCDA on Cu(111) the LUMO-derived interface state is more tightly bound than on Ag(111), the bonding distance is smaller, and the PTCDA molecule is distorted. Multiple layers of PTCDA on all three substrates have the same hole injection barrier since the work function of PTCDA monolayers is identical in all three cases.

## Acknowledgements

N.K. acknowledges financial support by the Emmy Noether-Program (DFG), F.S. and A.G. by the EPSRC and the DFG.

## References

- [1] A. Kahn, N. Koch, W.Y. Gao, *J. Polym. Sci. B* 41 (2003) 2529.
- [2] H. Ishii, K. Sugiyama, E. Ito, K. Seki, *Adv. Mater.* 11 (1999) 605.
- [3] N. Koch, A. Vollmer, *Appl. Phys. Lett.* 89 (2006) 162107.
- [4] H. Fukagawa, S. Kera, T. Kataoka, S. Hosoumi, Y. Watanabe, K. Kudo, N. Ueno, *Adv. Mater.* 19 (2007) 665.
- [5] X. Crispin, V. Geskin, A. Crispin, J. Cornil, R. Lazzaroni, W.R. Salaneck, J.-L. Bredas, *J. Am. Chem. Soc.* 124 (2002) 8131.
- [6] N. Koch, S. Duhm, J.P. Rabe, A. Vollmer, R.L. Johnson, *Phys. Rev. Lett.* 95 (2005) 237601.
- [7] N. Koch, A. Elschner, J. Schwartz, A. Kahn, *Appl. Phys. Lett.* 82 (2003) 2281.
- [8] G. Witte, S. Lukas, P.S. Bagus, C. Wöll, *Appl. Phys. Lett.* 87 (2005) 263502.
- [9] E. Ito, H. Oji, H. Ishii, K. Oichi, Y. Ouchi, K. Seki, *Chem. Phys. Lett.* 287 (1998) 137.
- [10] K. Seki, E. Ito, H. Ishii, *Synthetic Met.* 91 (1997) 137.
- [11] S. Kera, Y. Yabuuchi, H. Yamane, H. Setoyama, K.K. Okudaira, A. Kahn, N. Ueno, *Phys. Rev. B* 70 (2004) 085304.
- [12] S.K.M. Henze, O. Bauer, T.-L. Lee, M. Sokolowski, F.S. Tautz, *Surf. Sci.* 601 (2007) 1566.
- [13] A. Hauschild, K. Karki, B.C.C. Cowie, M. Rohlfling, F.S. Tautz, M. Sokolowski, *Phys. Rev. Lett.* 94 (2005) 036106.
- [14] A. Gerlach, S. Sellner, F. Schreiber, N. Koch, J. Zegenhagen, *Phys. Rev. B* 75 (2007) 045401.
- [15] Y. Zou, L. Kilian, A. Schöll, T. Schmidt, R. Fink, E. Umbach, *Surf. Sci.* 600 (2006) 1240.
- [16] M. Eremtchenko, D. Bauer, J.A. Schaefer, F.S. Tautz, *New J. Phys.* 6 (2004) 4.
- [17] Y. Hirose, A. Kahn, V. Aristov, P. Soukiassian, V. Bulovic, S.R. Forrest, *Phys. Rev. B* 54 (1996) 13748.
- [18] G. Gavrila, D.R.T. Zahn, W. Braun, *Appl. Phys. Lett.* 89 (2006) 162102.
- [19] I.G. Hill, A. Rajagopal, A. Kahn, Y. Hu, *Appl. Phys. Lett.* 73 (1998) 662.
- [20] E. Kawabe, H. Yamane, K. Koizumi, R. Sumii, K. Kanai, Y. Ouchi, K. Seki, *Mater. Res. Soc. Symp. Proc.* 965 (2007) S09.
- [21] R. Agrawal, S. Ghosh, *Appl. Phys. Lett.* 89 (2006) 222114.
- [22] P. Fenter, F. Schreiber, L. Zhou, P. Eisenberger, S.R. Forrest, *Phys. Rev. B* 56 (1997) 3046.
- [23] T. Schmitz-Hübsch, T. Fritz, F. Sellam, R. Staub, K. Leo, *Phys. Rev. B* 55 (1997) 7972.
- [24] N. Nicoara, E. Román, J.M. Gómez-Rodríguez, J.A. Martín-Gago, J. Méndez, *Org. Electron.* 7 (2006) 287.
- [25] M. Schneider, E. Umbach, M. Sokolowski, *Chem. Phys.* 325 (2006) 185.
- [26] V. Shklover, F.S. Tautz, R. Scholz, S. Sloboshanin, M. Sokolowski, J.A. Schaefer, E. Umbach, *Surf. Sci.* 454–456 (2000) 60.
- [27] T. Wagner, A. Bannani, C. Bobisch, H. Karacuban, M. Stöhr, M. Gabriel, R. Möller, *Org. Electron.* 5 (2004) 35.
- [28] T. Wagner, A. Bannani, C. Bobisch, H. Karacuban, R. Möller, *J. Phys. Condens. Mat.* 19 (2007) 056009.
- [29] B. Krause, A.C. Dürr, F. Schreiber, H. Dosch, O.H. Seeck, *J. Chem. Phys.* 119 (2003) 3429.

- [30] F.S. Tautz, M. Eremtchenko, J.A. Schaefer, M. Sokolowski, V. Shklover, E. Umbach, *Phys. Rev. B* 65 (2002) 125405.
- [31] E.V. Tsiper, Z.G. Soos, W. Gao, A. Kahn, *Chem. Phys. Lett.* 360 (2002) 47.
- [32] A. Schmidt, T.J. Schuerlein, G.E. Collins, N.R. Armstrong, *J. Phys. Chem.* 99 (1995) 11770.
- [33] R.L. Johnson, J. Reichardt, *Nucl. Instrum. Methods* 208 (1983) 791.
- [34] I.G. Hill, A. Kahn, Z.G. Soos, R.A. Pascal Jr., *Chem. Phys. Lett.* 327 (2000) 181.
- [35] N. Koch, G. Heimel, J. Wu, E. Zojer, R.L. Johnson, J.-L. Bredas, K. Müllen, J.P. Rabe, *Chem. Phys. Lett.* 413 (2005) 390.
- [36] I.G. Hill, A.J. Mäkinen, Z.H. Kafafi, *J. Appl. Phys.* 88 (2000) 889.
- [37] I. Chizhov, A. Kahn, G. Scoles, *J. Cryst. Growth* 208 (2000) 449.
- [38] L. Kilian, E. Umbach, M. Sokolowski, *Surf. Sci.* 600 (2006) 2633.
- [39] J. Kröger, H. Jensen, R. Berndt, R. Rurai, N. Lorente, *Chem. Phys. Lett.* 438 (2007) 249.
- [40] N. Koch, S. Duhm, J.P. Rabe, S. Rentenberger, R.L. Johnson, J. Klankermayer, F. Schreiber, *Appl. Phys. Lett.* 87 (2005) 101905.
- [41] S. Duhm, H. Glowatzki, V. Cimpeanu, J. Klankermayer, J.P. Rabe, R.L. Johnson, N. Koch, *J. Phys. Chem. B* 110 (2006) 21069.
- [42] H. Vázquez, R. Oszwaldowski, P. Pou, J. Ortega, R. Pérez, F. Flores, A. Kahn, *Europhys. Lett.* 65 (2004) 802.
- [43] B. Krause, A.C. Dürr, K. Ritley, F. Schreiber, H. Dosch, D. Smilgies, *Phys. Rev. B* 66 (2002) 235404.
- [44] B. Krause, F. Schreiber, H. Dosch, A. Pimpinelli, O.H. Seeck, *Europhys. Lett.* 65 (2004) 372.
- [45] M. Möbus, N. Karl, T. Kobayashi, *J. Cryst. Growth* 116 (1992) 495.
- [46] I.G. Hill, A. Kahn, *J. Appl. Phys.* 84 (1998) 5583.
- [47] H. Vázquez, W. Gao, F. Flores, A. Kahn, *Phys. Rev. B* 71 (2005) 041306.